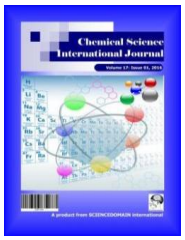

Chemical Science International Journal
18(3): 1-9, 2017; Article no.CSIJ.32444
Previously known as American Chemical Science Journal
ISSN: 2249-0205

SCIENCEDOMAIN *international*
www.sciencedomain.org

Green Remediation of Carbamazepine from Water Using Novel Magnetic Iron Modified Carbonized Baggasse: Kinetics, Equilibrium and Mechanistic Studies

Selly Jemutai-Kimosop[1*], Veronica A. Okello[2], Francis Orata[1], Zachary M. Getenga[3] and Victor O. Shikuku[4]

[1]Masinde Muliro University of Science and Technology, P.O.Box 190, Kakamega, Kenya.
[2]Machakos University, P.O.Box 136-90100, Machakos, Kenya.
[3]Chuka University, P.O.Box 109-60400, Chuka, Kenya.
[4]Maseno University, Private Bag, Maseno, Kenya.

Authors' contributions

This work was carried out in collaboration between all authors. Authors SJK and VOS designed the experimental work, performed the statistical analysis, wrote the protocol and wrote the first draft of the manuscript. Authors VAO, FO and ZMG developed the study concept, supervised the study and development of the manuscripts from the study. All authors read and approved the final manuscript.

Article Information

DOI: 10.9734/CSJI/2017/32444
Editor(s):
(1) Zygadlo Julio Alberto, Professor of Chemistry, National University of Cordoba, Argentina.
Reviewers:
(1) Vito Rizzi, University of Bari, Italy.
(2) Sinem Gokturk, Marmara University, Turkey.
Complete Peer review History: http://www.sciencedomain.org/review-history/18207

Original Research Article

Received 26th February 2017
Accepted 7th March 2017
Published 15th March 2017

ABSTRACT

Baggasse derived biochar magnetically modified with iron (α-Fe_2O_3-CBG) was fabricated, characterized and applied as a low-cost adsorbent for the removal of carbamazepine (CBZ), a pharmaceutically active compound which has been reported as an emergent water contaminant. Characterization of the synthesized (α-Fe_2O_3-CBG) composite showed that iron was effectively impregnated onto the carbonized bagasse network. The composite was able to achieve 60.9 % CBZ removal within a period of 4 hours. The time-dependency adsorption data followed the pseudo-second order kinetic law while the intraparticle diffusion model indicated that pore diffusion is not the

**Corresponding author: E-mail: skimosop@mmust.ac.ke;*

sole operative rate-determining mechanism with significant boundary layer effects. Freundlich model best explained the equilibrium sorption data. The adsorption extent was also strongly pH-dependent though adsorption mechanism is significantly driven by electrostatic interactions at lower pH. Furthermore, magnetic separation of the contaminant-laden adsorbent was successfully accomplished.

Keywords: Carbamazepine; adsorption; water; magnetic; iron-oxide.

1. INTRODUCTION

Pharmaceuticals compounds (PCs) are a group of emerging contaminants and their use is continuously increasing globally. They are extensively used in human and veterinary medicine in disease control and treatment. Pharmaceuticals and their metabolites are readily excreted with urine and faeces and enter into urban wastewater treatment plants (WWTPs) [1]. These compounds also find their way into the aquatic environment through discharge of treated wastewater, seepage from landfills, septic systems, sewer lines and disposal of expired drugs into water systems among other pathways [2]. Consequently, a wide range of PCs have been detected in a variety of environmental samples such as wastewater and drinking water [3]. Reports indicate the accumulation of some pharmaceuticals in sewage sludge [4], while other studies show the presence of pharmaceutically active ingredients in public drinking water wells where septic systems are prevalent [5]. The presence of PCs in aquatic environment is of great concern since they have explicitly been shown to be toxic to aquatic organisms and may induce development of drug resistant bacteria [6].

Current studies show that effluents from wastewater treatment plants contain xenobiotic organic compounds which can have a lot of ecotoxicological effects thus impacting negatively on environmental systems [7]. Carbamazepine, benzo[b][1]benzazepine-11-carboxamide, a human pharmaceutical for treating epileptic seizures, trigeminal neuralgia, bipolar depression, excited psychosis, and mania [8] is not degraded in WWTP processes due to its resistance to microbial biodegradation and thus most removal efficiencies are below 10% [9]. Sorption of carbamazepine onto sewage sludge is not an effective removal pathway because of the low affinity for organic matter (K_d = 1.2 L/kg). Consequently, carbamazepine is commonly found in WWTP effluents. Studies have reported carbamazepine in effluent at concentrations up to 1.6 µg/L [10,11]. Studies by [12] show the toxicity of carbamazepine to aquatic insects. Carbamazepine degradation products such as aza-arenes may be toxic and potentially carcinogenic [13]. There is need for continuous evaluation of alternative strategies for removal of PCs from water. Agricultural wastes biomass present suitable precursors for adsorbent preparation due to their abundance hence low capital investment besides their demonstrated efficacy to remove selected PCs from water [14].

The objective of this study was to investigate the adsorptive features of iron-modified carbonized baggasse (α-Fe_2O_3-CBG) for removal of carbamazepine (CBZ) from water. Iron modification was intended to induce magnetic properties to the adsorbent improving adsorbent removal by external magnetic field. The effect of contact time, initial adsorbate concentration, adsorbent and solution pH under batch conditions are herein discussed. The study also investigated the possible adsorption mechanisms governing the adsorption process.

2. MATERIALS AND METHODS

2.1 Chemicals and Materials

High purity carbamazepine standard was purchased from Sigma Aldrich, Germany. Analytical grade and HPLC grade water and acetonitrile for analysis were purchased from Sigma Aldrich through Kobian Kenya Limited. Syringe filters were obtained from Estec Kenya Limited. All stock solutions were prepared using HPLC grade acetonitrile and working standards diluted with HPLC water. Sugarcane baggasse was obtained from local millers.

2.2 Adsorbent Preparation

The biomass for generation of biochar was baggasse from Nzoia Sugar Company, Kenya. The carbonized baggasse (CBG) was prepared as described in our previous work [14]. In brief, the biomass was chopped into pieces then thoroughly washed with de-ionized (DI) water to remove all adhering dirt and air dried before

pyrolysis. Carbonization was achieved by slow-pyrolysis at 350°C and at a heating rate of 10°C minute^{-1} and a residence time of 1 h in the reactor. The biochar was then washed with DI water until the effluent from it was neutral to litmus and oven-dried at 100°C for 2 h. Iron modified carbonized baggasse (α-Fe_2O_3-CBG) was then fabricated by direct hydrolysis of an iron salt following the protocol described by [15] with slight modification. Iron salt solution prepared by dissolving 10 g of $FeCl_3.4H_2O$ in 50 mL of DI water were mixed with 10g of CBG for 8 h under continuous agitation and finally oven dried at 100-120°C for 12 h. The resultant product, iron modified carbonized baggasse (α-Fe_2O_3-CBG), was sieved to obtain uniform particle size (< 220 µm) then stored in air-tight containers for adsorption experiments.

2.3 Kinetics Studies Experiments

The kinetics experiments were performed by batch technique. 0.1 g of the adsorbent (α-Fe_2O_3-CBG) was dispersed into 250 mL conical glass flasks containing 1 mg L^{-1} CBZ in 50 mL solution at 298 K and agitated at 120 rpm using an overhead temperature-controlled shaker (GFL-3006). At pre-determined regular time intervals (0, 0.5, 1, 2, 3, 4, 5, 6 hrs) 0.5 mL aliquots was withdrawn and filtered through 0.22 µm syringe filters into sealed glass vials for residual CBZ analysis.

Carbamezapine was detected by HPLC with UV detection (Shimadzu LC 20AT) at 252 nm. The mobile phase was a mixture of acetonitrile and water (70:30 v/v), with a flow rate of 1 mL min^{-1}. The injection volume was 20 µL.

The amount of CBZ adsorbed per unit mass at pre-equilibrium time (t) was obtained by equation 1:

$$q_t = \frac{(C_i - C_e)V}{m} \quad (1)$$

Where, C_i and C_e are the initial and equilibrium concentration (mg L^{-1}), m is the mass of adsorbent (g) and V the volume of the solution (L). To obtain the kinetic parameters, the kinetic data was fitted to three widely used kinetic models, *viz*. pseudo-first order [16], pseudo-second-order [17], and intra-particle diffusion models [18] represented in the equations 2,3 and 4 below:

Pseudo-first-order model:

$$\log (q_e - q_t) = \log q_e - \frac{k_1 t}{2.303} \quad (2)$$

Pseudo-second-order model:

$$\frac{t}{q_t} = \frac{1}{k_2 (q_e)^2} + \frac{t}{q_e} \quad (3)$$

Intraparticle diffusion model:

$$q_t = k_p t^{0.5} + C \quad (4)$$

2.4 Adsorption Isotherm Experiments

Adsorption isotherms for CBZ onto α-Fe_2O_3-CBG were determined using 0.1g iron-impregnated biochar with 50 mL CBZ solutions of varied concentrations (0.25, 0.5, 0.75, 1.00 and 1.25 mgL^{1}) in a batch mode. The vessels were agitated under similar experimental conditions as in the kinetics experiments described in section 2.3 until equilibration as determined from the kinetic experiments (4 h). The amount of solute adsorbed per unit mass of adsorbent at equilibrium (q_e) was calculated using equation 5:

$$q_e = \frac{(C_i - C_e)V}{m} \quad (5)$$

The equilibrium sorption data was modeled using linearized Langmuir and Freundlich isotherm equations shown in Table 1 and the isotherm parameters calculated.

Table 1. The linearized isotherm equations and parameters

Isotherm Model	Equation	Parameters	Reference
Langmuir	$\frac{1}{q_e} = \frac{1}{Q_o} + \frac{1}{Q_o K_L C_e}$	Q_o (mg/g), K_L (L/g)	[19]
Freundlich	$\log q_e = \log K_f + \frac{1}{n} \log C_e$	K_f, n	[20]

2.5 Effect of pH

The effect of pH on the extent of CBZ removal was investigated over a pH range of 2-10. Here, 50 mL (1 mg L^{-1}) of CBZ solution and 0.1 g α-Fe_2O_3-CBG was placed in glass conical flask and 1 M HCl and 1 M NaOH solutions were used for initial pH adjustment. The solutions were then agitated at120 rpm at 298 K until equilibration. The pH was measured using a pH meter (MrC 86505, scientific instrument).

3. RESULTS AND DISCUSSION

3.1 Adsorbent Characterization

The elemental composition of the unmodified carbonized baggasse and iron-modified biochar (α-Fe_2O_3-CBG) obtained from XRF (Table 2) indicate successful impregnation of iron into the biochar. XRD data (supplementary material) showed haematite (α-Fe_2O_3) as the only crystallized iron phase in the modified biochar, with diffraction peaks at 2θ = 24.1°, 33.1°, 35.60°, 39.1°, 40.9°, 43.4°, 40.9°, 49.4°, 54.0°. Other forms of magnetic minerals possibly formed during sythesis, *viz*, magnetite (Fe_3O_4) and maghemite (γ-Fe_2O_3), were converted to haematite under thermal treatment [21] with concomitant leaching of other elements in solution. The other prominent crystalline phase in α-Fe_2O_3-CBG was quartz (SiO_2).

Table 2. Elemental composition of unmodified and modified carbonized baggasse

Major elements	Adsorbent materials (wt %)	
	Unmodified biochar	α-Fe_2O_3-CBG
Ca	37.52	0.71
K	27.52	0.87
Fe	18.52	78.80
Mn	5.49	0.21
Zn	0.82	0.20

The functional groups present in the prepared adsorbent according to transmittance near IR (400-4000 cm^{-1}) analysis are displayed in Fig. 1. The bands at 3300-3600 cm^{-1} were assigned to both free and hydrogen bonded –OH stretching vibrations due to phenolic functions. The peaks in the 1700-1600 cm^{-1} region were ascribed to C=O stretching vibrations resulting from ketones, carboxylic acids, anhydrides and esters (Mohan et al. 2014). The peaks in the region 1500-1400 cm^{-1} were attributed to the presence of inorganic functional groups such as alumina-silicates and metal oxides [22]. The bands centered in the region 700- 500 cm^{-1} are characteristic absorption bands of Fe–O bonds suggesting successful incorporation of iron oxides as testified by XRD analyses [23].

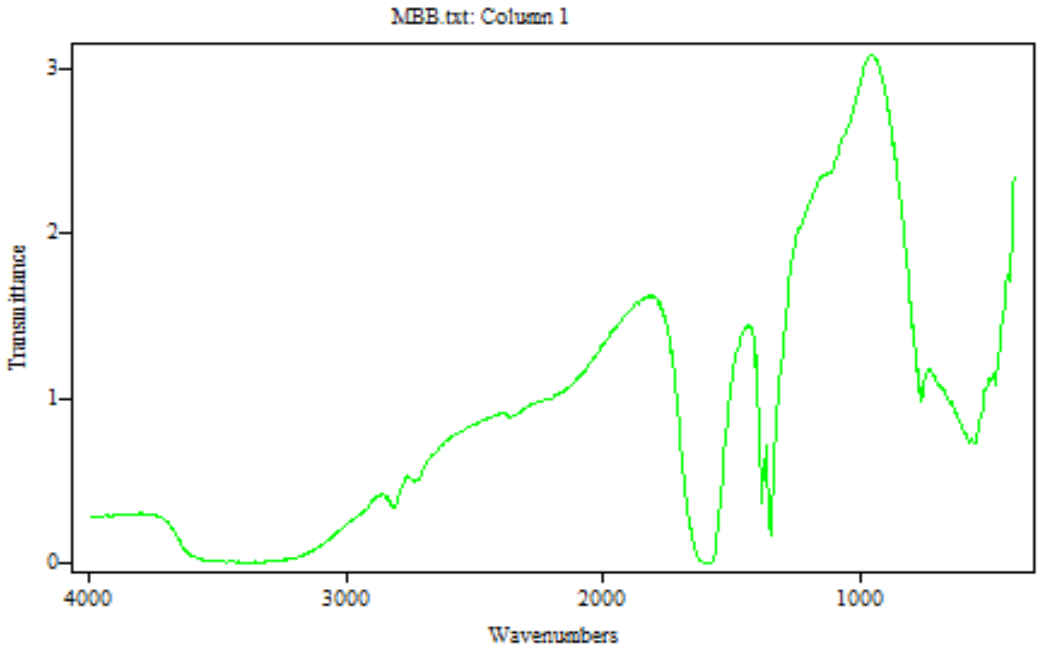

Fig. 1. FT-IR spectrum for the iron modified baggase biochar (α-Fe_2O_3-CBG)

3.2 Effect of Contact Time

The removal of carbamazepine (CBZ) by the α-Fe_2O_3-CBG as a function of time depicted relatively fast adsorption kinetics leading to saturation within 240 min (Fig. 2) followed by a slow phase with no appreciable change, implying pseudo-equilibrium conditions. This is due to availability of large number of vacant adsorption sites at the onset. Accessibility to these sites becomes sequentially limited following occupancy by the CBZ molecules thus the system achieves equilibrium.

In order to predict the adsorption rate and nature of the rate-controlling step(s), the kinetic data were simulated using pseudo-first order and pseudo-second order kinetic models. The applicability of the model was evaluated by the linear regression coefficient (R^2) values and the closeness between experimental equilibrium adsorption capacity (q_{exp}) and the theoretical values (q_{cal}) obtained from the kinetic models. The pseudo-first order posted poor fitting to the experimental data indicating the adsorption of carbamazepine onto α-Fe_2O_3-CBG is not a first-order reaction. On the other hand, the pseudo-second-order kinetic model best simulated the adsorption of CBZ onto α-Fe_2O_3-CBG (Fig. 3) with high R^2 (0.998) value corroborated with the convergence of the calculated (q_{cal}) and experimental (q_{exp}) adsorption capacities, implying the rate controlling step is a chemisorption process involving exchange of valence electrons (Table 3).

The nature of the rate controlling step and the transport mechanism of adsorbate molecules through the bulk solution to the adsorbent binding sites were evaluated by fitting the data to the intra-particle diffusion model (equation 4). Theoretically, if the regression plot of q_t versus $t^{0.5}$ is linear, then intraparticle diffusion occurs. If the plot has a zero y-intercept then intraparticle pore transport is the sole operating rate controlling mechanism. Otherwise (c >0), multiple steps are involved in the rate-determining step. In the present work, the pre-equilibrium adsorption (q_t) had a relatively high linear dependency on $t^{0.5}$ (R^2=0.941) depicting a strong influence of intraparticle diffusion process. Nevertheless, the plot did not pass through the origin (Fig. 4) implying that pore transport is not the only rate controlling mechanism; hence other adsorption sequences are involved. Relative to the pre-equilibrium adsorption, the linear plot had significant intercept (Table 3) suggesting significant boundary layer effects attributable to a wide distribution of pore sizes [14].

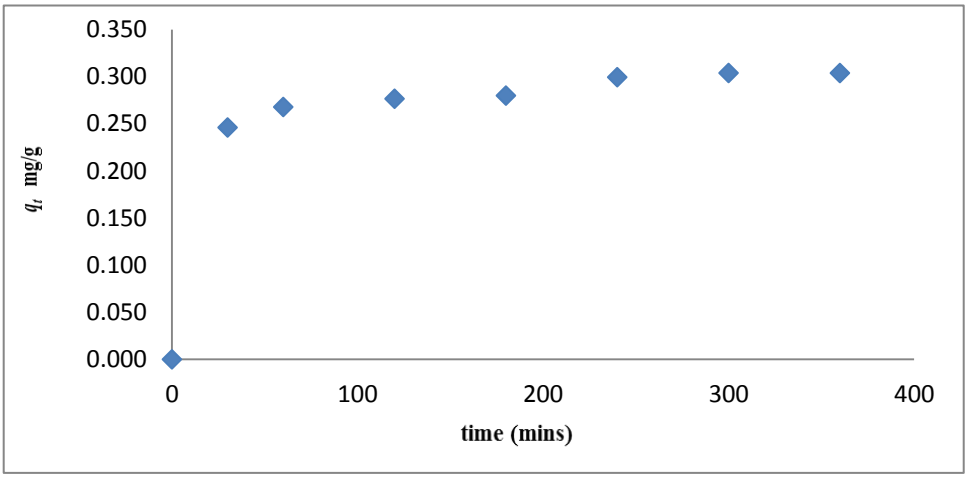

Fig. 2. Effect of contact time for CBZ adsorption onto α-Fe_2O_3-CBG composite

Table 3. Pseudo-second order and intraparticle diffusion model parameters for CBZ adsorption onto α-Fe_2O_3-CBG

Pseudo-second order parameters		Intraparticle diffusion model parameters	
$q_{e(exp)}$	0.3015 mg/g	$q_{e(exp)}$	0.3015 mg/g
$q_{e(cal)}$	0.3132 mg/g	k_p	0.004
k_2	0.2563 g mg^{-1} min^{-1}	C	0.228 mg/g
R^2	0.998	R^2	0.941

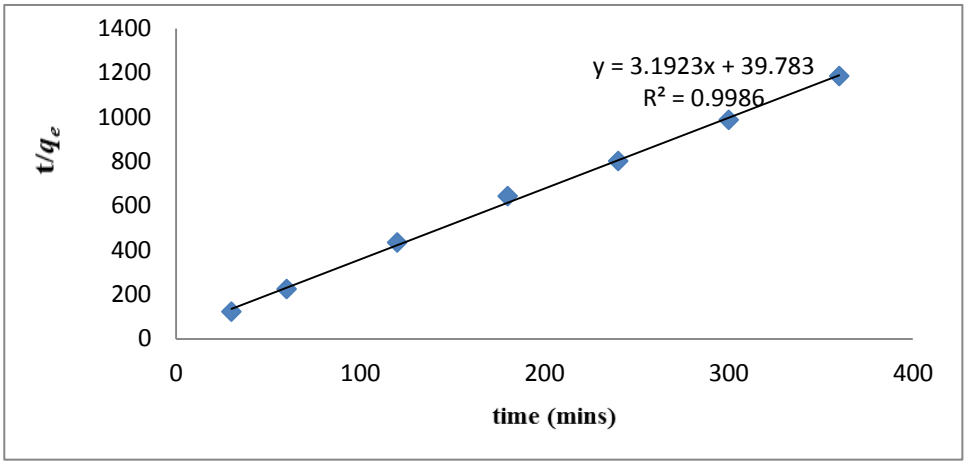

Fig. 3. Pseudo-second order kinetic plot for CBZ adsorption onto α-Fe_2O_3-CBG

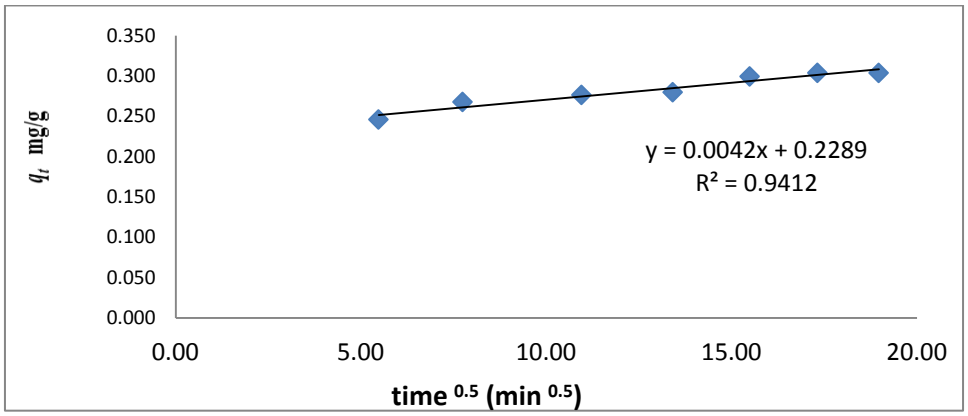

Fig. 4. Intraparticle diffusion model plot for CBZ adsorption onto α-Fe_2O_3-CBG

3.3 Effect of Initial Concentration

The removal extent of CBZ by α-Fe_2O_3-CBG in percentage was found to increase from ca. 42.9% to ca. 60.9% when the initial concentration was raised from 0.5 to 1.0 mg/L for adsorbent dosage of 0.1 g/50 mL beyond which a decrease is noted. The initial increase indicates that mass gradient serves as the driving force for the adsorption process. As observed in the evolution of distribution coefficient (K_d) as a function of initial concentration (Fig. 5), the increase in K_d with increase in adsorbate concentration imply availability of more energetically favored sites for adsorption [24]. The gradual decrease beyond 1 mg/L is due to saturation of the active binding sites with concomitant repulsion between the adsorbates at high concentration.

3.4 Isotherm Modeling

To investigate the distribution of the adsorbates over the liquid-solid phases, the equilibrium data as a function of initial concentration were fitted to two well-known adsorption isotherms, namely Langmuir and Freundlich isotherms and the computed parameters are shown in Table 4. Both isotherm models posted relatively low linear correlation coefficients (R^2), implying each individual model could not completely describe the adsorption mechanism suggesting multi-mechanistic adsorption sequences. However, the data tended to conform to the Freundlich model. Furthermore, besides the low R^2 values, the negative Langmuir isotherm constants (Q_o and K_L) values are unacceptable for they bear no physical meaning. This indicates that the inherent postulates of this model cannot satisfactorily explain the adsorption mechanism of carbamazepine onto α-Fe_2O_3-CBG [25]. Therefore, rationally, despite the relatively low R^2 value, the adsorption of CBZ onto α-Fe_2O_3-CBG could be explained in terms of Freundlich isotherm model. The magnitude of Freundlich constant n was less than unity indicating poor adsorptive character while 1/n is above unity corroborating the aforementioned cooperative

adsorption constituting several mechanisms [26, 27].

3.5 Effect of pH and Adsorption Mechanism

The pH dependence was studied in the range 2.0 to12.0. The adsorption of CBZ was strongly pH dependent with maximum adsorption at pH 6 for CBZ (Fig. 6).

The variation of adsorption capacities with pH gives insight on the possible interaction mechanisms involved. CBZ has two pK_a values because it dissociates at two different functional groups depending on the pH. These are pK_a at 2.30 (ketone group) and 13.90 (amine group) for CBZ [28]. Therefore, below pH 2.3, CBZ was a positively charged species (CBZ^+) and electrostatic repulsion becomes significant and accounts for the decreased adsorption capacity observed. However, throughout the pH range, CBZ were neutrally charged species (CBZ^0) and the effect of electrostatic interactions was negligible and can be neglected and hence other adsorption mechanisms besides electrostatic interactions such as hydrophobic interactions play key role. These results indicate that the pH-dependent speciation of the compounds largely controls their adsorption mechanism and the retention mechanism involves, in part, non-electrostatic driven interactions.

Table 4. Calculated adsorption isotherm parameters

Isotherm model	Parameters
Freundlich	R^2=0.808 n=0.5373 k_f=1.4256 L/mg
Langmuir	R^2=0.758 Q_0=-0.1806 mg/g K_L=-1.4525 L/mg

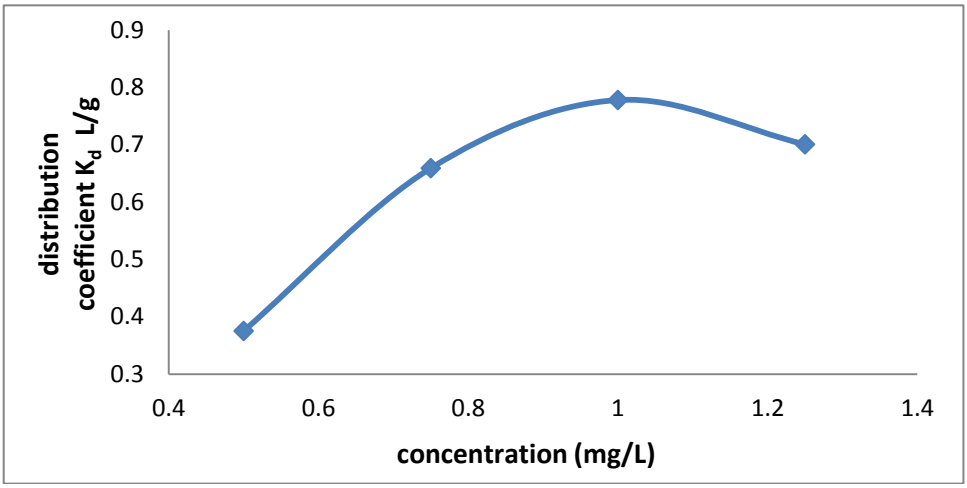

Fig. 5. Evolution of CBZ distribution coefficient (K_d) as function of initial concentration

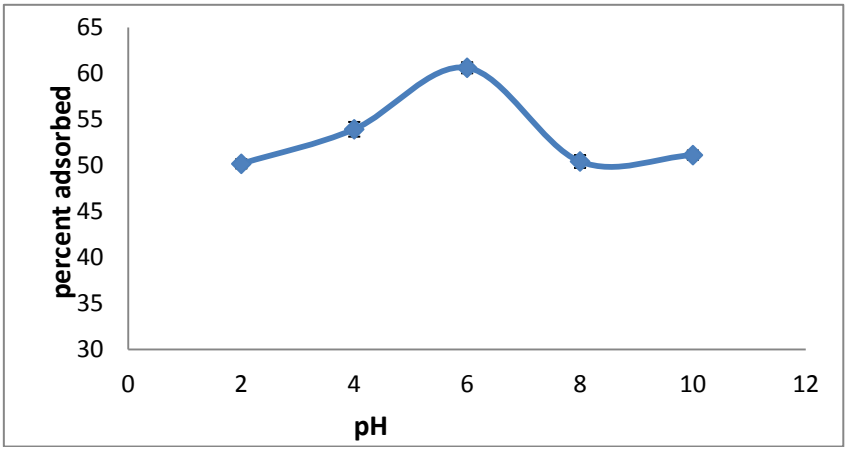

Fig. 6. pH dependence plot for CBZ adsorption onto α-Fe_2O_3-CBG

4. CONCLUSION

A novel engineered α-Fe_2O_3-CBG adsorbent was developed by magnetic modification of carbonized bagasse. The composite achieved an absorption capacity of 60.9% CBZ. The optimum adsorption was achieved at pH -6 and a temperature of 25°C. This study demonstrated that iron modified carbonized baggasse (α-Fe_2O_3-CBG) composite presents a potential precursor for development of magnetically responsive carbonaceous adsorbent for removal of carbamazepine from aqueous media. The Equilibrium data was describable by the Freundlich isotherm model. The adsorption kinetic data followed the pseudo-second-order model while intraparticle diffusion model showed that pore transport was not the only rate-determining mechanism. The pH dependence studies indicated that electrostatic interactions dominantly drive the adsorption mechanism and adsorption extent.

ACKNOWLEDGEMENTS

The authors are grateful to Dr. Dickson Andala for assistance in adsorbent characterization.

COMPETING INTERESTS

Authors have declared that no competing interests exist.

REFERENCES

1. Ellis JB. Antiviral pandemic risk assessment for urban receiving waters. Water Science and Technology. 2010; 61(4):879-884.
2. González-Naranjo V, Boltes K, Biel M. Mobility of ibuprofen, a persistent active drug, in soils irrigated with reclaimed water. Plant Soil Environ. 2013;59(2):68–73.
3. Cai MQ, Wang R, Feng L, Zhang LQ. Determination of selected pharmaceuticals in tap water and drinking water treatment plant by high-performance liquid chromatography-triple quadrupole mass spectrometer in Beijing, China. Environmental Science and Pollution Research. 2014;1-14.
4. Jelic A, Gros M, Ginebreda A, Cespedes-Sánchez R, Ventura F, Petrovic M, Barceló D. Occurrence, partition and removal of pharmaceuticals in sewage water and sludge during wastewater treatment. Water Res; 2011.
5. Schaider LA, Ruthann AR, Ackerman JM, Dunagan SC, Brody JG. Pharmaceuticals, perfluorosurfactants and other organic wastewater compounds in public drinking water wells in a shallow sand and gravel aquifer. Sci. Total Environ. 2014;468–469: 384–393.
6. Li WC. Occurrence, sources and fate of pharmaceuticals in aquatic environment and soil. A review. Environ. Poll. 2014; 187:193-201.
7. Kimosop SJ, Getenga ZM, Orata FO, Okello VA, Cheruiyot JK. Residue levels and discharge loads of antibiotics in wastewater treatment plants and hospital lagoons within Lake Victoria Basin, Kenya. Journal of Environmental Monitoring and Assessment. 2016;188:532.
DOI: 10.1007/s10661-016-5534-6
8. Thacker PD. Pharmaceutical data elude researchers. Environ Sci Technol. 2005; 39:193A-194A.
9. Zhang Y, Geißen SU, Gal C. Carbamazepine and diclofenac: Removal in wastewater treatment plants and occurrence in water bodies. Chemosphere. 2008;73(8):1151-1161.
10. Heberer T, Reddersen K, Mechlinski A. From municipal sewage to drinking water: Fate and removal of pharmaceutical residues in the aquatic environment in urban areas. Water Sci. Technol. 2002; 46:81–88.
11. Glassmeyer ST, Furlong ET, Kolpin DW, Cahill JD, Zaugg SD, Werner SL. Transport of chemical and microbial contaminants from known wastewater discharge: Potential for use as indicators of human fecal contamination. Environmental Science and Technology. 2005;36:5157–69.
12. Oetken M, Nentwig G, Loffler D, Ternes T, Oehlmann J. Effects of pharmaceuticals on aquatic invertebrates. Part I. The antiepileptic drug carbamazepine. Arch Environ Contam Toxicol. 2005;49:353-361.
13. Kosjek T, Andersen HR, Kompare B, Ledin A, Heath E. Fate of carbamazepine during water treatment. Environ Sci Technol. 2009;43:6256-6261.
14. Ng'eno E, Orata F, Lilechi DB, Shikuku VO, Kimosop S. Adsorption of caffeine and ciprofloxacin onto pyrolytically derived water hyacinth biochar: Isothermal, kinetics and thermodynamics. Journal of Chemistry

and Chemical Engineering. 2016;10:185-194.
15. Hu X, Zhuhong D, Zimmerman R, Wang S, Gao B. Batch and column adsorption of arsenic onto iron-impregnated biochar synthesized through hydrolysis. Water Res. 2015;68:206-216.
16. Ho YS, McKay G. Sorption of dye from aqueous solution by peat. Chem. Eng. J. 1998;70:115–124.
17. Ho YS. Review of second-order models for adsorption systems. J. Hazard. Mater. 2006;136:681-689.
18. Weber WJ, Morris JC. Kinetics of adsorption on carbon from solution. J. San. Eng.: Am. Soc. Civ. Eng. 1963;89: 31-59.
19. Langmuir I. The constitution and fundamental properties of solids and liquids. J. Am. Chem. Soc. 1916;38:2221–2295.
20. Freundlich HMF. U¨ ber die adsorption in lo¨sungen. Z. Phys. Chem. 1906;57:385–470.
21. Shikuku VO, Winfrida N. Nyairo, Chrispin O. Kowenje. Fundamentals and sources of magnetic nanocomposites and their sorption properties: In Tawfik A. Saleh (Editor) Advanced Nanomaterials for Water Engineering, Treatment and Hydraulics. IGI Global Publishers. 2017;64.
ISBN: 13: 9781522521365
22. Jin H, Sergio C, Zhizhou C, Jun G, Yueding X, Jianying Z. Biochar pyrolytically produced from municipal solid wastes for aqueous As(V) removal: Adsorption property and its improvement with KOH activation. Bioresource Technology. 2014; 169:622–629.
23. Ercuta A, Chirita M. Highly crystalline porous magnetite and vacancy-ordered maghemite microcrystals of rhombohedral habit. J. Crystal Growth. 2013;380:182–186.
24. Shikuku VO, Kowenje CO, Ongeri DMK, Zanella R, Prestes OD. Removal of tebuconazole from wastewater by zeolite X: Kinetics and thermodynamics studies. International Journal of Engineering, Research and Technology. 2014;3(8):584-1590.
25. Shikuku VO, Filipe F. Donato, Kowenje CO, Zanella R, Prestes OD. A comparison of adsorption equilibrium, kinetics and thermodynamics of aqueous phase clomazone between Faujasite X and a Natural Zeolite from Kenya. South Africa Journal of Chemistry. 2015;68:245–252.
26. Saleh TA. Isotherm, kinetic, and thermodynamics studies on Hg (II) adsorption from aqueous solution by silica-multiwall carbon nanotubes. Environ Sci Pollut Res. 2015;22:16721-16731.
27. Treybal RE. Mass-transfer operations. 3rd ed., McGraw-Hill; 1981.
28. Punyapalakul P, Sitthisorn T. Removal of ciprofloxazin and carbamazepine by adsorption on functionalized mesoporous silicates. World Academy of Science, Engineering and Technology. 2010;69: 546-550.

Peer-review history:
The peer review history for this paper can be accessed here:
http://sciencedomain.org/review-history/18207